Experimental Cell Research 433 (2023) 113820

Contents lists available at ScienceDirect

Experimental Cell Research

journal homepage: www.elsevier.com/locate/yexcr

Research article

Myotube growth is associated with cancer-like metabolic reprogramming and is limited by phosphoglycerate dehydrogenase

Lian E.M. Stadhouders [a], Jonathon A.B. Smith [b,c,1], Brendan M. Gabriel [d,2], Sander A. J. Verbrugge [e], Tim D. Hammersen [a], Detmar Kolijn [a,f], Ilse S.P. Vogel [a], Abdalla D. Mohamed [b,g], Gerard M.J. de Wit [a], Carla Offringa [a], Willem M.H. Hoogaars [a], Sebastian Gehlert [h,i], Henning Wackerhage [e,3], Richard T. Jaspers [a,*,3]

[a] Laboratory for Myology, Department of Human Movement Sciences, Faculty of Behavioural and Movement Sciences, Vrije Universiteit Amsterdam, Amsterdam Movement Sciences, De Boelelaan 1108, 1081 HZ, Amsterdam, the Netherlands
[b] School of Medicine, Medical Sciences and Nutrition, University of Aberdeen, Foresterhill, Aberdeen, AB25 2ZD, UK
[c] Department of Physiology and Pharmacology (FYFA), Group of Integrative Physiology, Karolinska Institutet, Stockholm, Sweden
[d] Aberdeen Cardiovascular & Diabetes Centre, The Rowett Institute, University of Aberdeen, Aberdeen, UK
[e] Exercise Biology, Department for Sport and Health Sciences, Technical University of Munich, Georg-Brauchle-Ring 60/62, 80992, München/Munich, Germany
[f] Department of Clinical Pharmacology and Molecular Cardiology, Ruhr University Bochum, Bochum, Germany
[g] Cancer Therapeutics Unit, Target Genomic and Chromosomal Instability, The Institute of Cancer Research, 15 Cotswold Road, Sutton, London, SM2 5NG, UK
[h] Department for the Biosciences of Sports, Institute of Sports Science, University of Hildesheim, Universitätsplatz 1, 31141, Hildesheim, Germany
[i] Department for Molecular and Cellular Sports Medicine, German Sport University Cologne, 50933, Cologne, Germany

ARTICLE INFO

Keywords:
Glycolysis
Hypertrophy
Insulin-like growth factor I
Metabolism
Skeletal muscle
Warburg effect

ABSTRACT

The Warburg effect links growth and glycolysis in cancer. A key purpose of the Warburg effect is to generate glycolytic intermediates for anabolic reactions, such as nucleotides → RNA/DNA and amino acids → protein synthesis. The aim of this study was to investigate whether a similar 'glycolysis-for-anabolism' metabolic reprogramming also occurs in hypertrophying skeletal muscle. To interrogate this, we first induced C2C12 myotube hypertrophy with IGF-1. We then added ^{14}C glucose to the differentiation medium and measured radioactivity in isolated protein and RNA to establish whether ^{14}C had entered anabolism. We found that especially protein became radioactive, suggesting a glucose → glycolytic intermediates → non-essential amino acid(s) → protein series of reactions, the rate of which was increased by IGF-1. Next, to investigate the importance of glycolytic flux and non-essential amino acid synthesis for myotube hypertrophy, we exposed C2C12 and primary mouse myotubes to the glycolysis inhibitor 2-Deoxy-D-glucose (2DG). We found that inhibiting glycolysis lowered C2C12 and primary myotube size. Similarly, siRNA silencing of PHGDH, the key enzyme of the serine biosynthesis pathway, decreased C2C12 and primary myotube size; whereas retroviral PHGDH overexpression increased C2C12 myotube size. Together these results suggest that glycolysis is important for hypertrophying myotubes, which reprogram their metabolism to facilitate anabolism, similar to cancer cells.

1. Introduction

Having sufficient muscle mass and strength is associated with low morbidity and mortality [1,2]. An individual's muscle mass and strength depends on both genetics [3,4] and environmental factors. Of the environmental factors, resistance (strength) training increases muscle mass and strength in most individuals [5]. Resistance training increases muscle mass by elevating protein synthesis for 48 [6] to 72 [7] hours post-exercise, resulting in a positive protein balance in fed individuals. The main mechanism by which resistance exercise increases protein

* Corresponding author.
E-mail address: r.t.jaspers@vu.nl (R.T. Jaspers).
[1] Present address.
[2] Affiliated to research: Department of Physiology and Pharmacology (FYFA), Group of Integrative Physiology, Karolinska Institutet, Solnavägen 9, 171 65 Solna, Sweden.
[3] shared last author.

https://doi.org/10.1016/j.yexcr.2023.113820
Received 30 June 2022; Received in revised form 10 October 2023; Accepted 14 October 2023
Available online 23 October 2023

synthesis is the activation of the serine/threonine kinase mTOR, which is part of the mTORC1 complex [8]. In addition, hypertrophy-inducing stimuli such as synergist ablation [9] and acute resistance exercise [10,11] extensively change gene expression. The transcription factor *MYC* is one of the most robustly changed transcripts, increasing >10-fold in synergist-ablated hypertrophying mouse plantaris [9] and ≈6-fold 2.5 h after resistance exercise in human vastus lateralis muscle [10,11].

Both *MTOR* and *MYC* are cancer genes [12] and one of their functions is to contribute to the metabolic reprogramming seen in cancer cells [13]. Nearly 100 years ago, the metabolic reprograming of cancer cells was first experimentally demonstrated by Otto Warburg [14]. In a key experiment, the Warburg group compared glucose uptake and lactate production of sarcomas with those of healthy organs in rats. They noted that sarcomas took up more glucose and produced more lactate than other organs, such as the liver, kidney, or brain [14]. This demonstrated that cancer cells take up more glucose and have a higher glycolytic flux in the presence of oxygen. This phenomenon was termed the 'Warburg effect' by Efraim Racker, in contrast to anaerobic glycolysis (also known as the 'Pasteur effect') [15]. The purpose of the metabolic reprogramming of cancer cells was long poorly understood. Today we know that the pathways affected by metabolic reprogramming vary greatly between different types of cancer [16], and that a key function of this metabolic reprogramming is to shunt glycolytic intermediates and other metabolites into anabolic reactions. These anabolic reactions include amino acids into protein and nucleotides into RNA/DNA synthesis, which enables cancer cells to produce the biomass necessary for growth and proliferation [13].

Given that the metabolic reprograming regulator mTORC1 is active and that *MYC* is highly expressed in hypertrophying muscle, the question arises: Do hypertrophying skeletal muscle fibres reprogram their metabolism to support growth in a similar way to cancer cells? Several lines of evidence support this idea [17]. First, resistance exercise not only increases protein synthesis [6] but also glucose uptake for at least one day post-exercise [18,19]. Second, Semsarian et al. noted that IGF-1-induced hypertrophy of C2C12 myotubes was associated with increased lactate production and an elevated expression of lactate dehydrogenase [20], which is essentially the Warburg effect. Similarly, muscle activation of AKT1, a known cancer metabolism regulator [21], not only causes hypertrophy but also increases the expression of glycolytic enzymes [22]. Similarly, mTORC1 activation, through loss of its inhibitor NPRL2, results in muscle hypertrophy and induces aerobic glycolysis in mice [23]. Finally, a loss of myostatin both induces muscle hypertrophy and promotes a shift towards a more glycolytic metabolism [24]. Collectively, these data suggest that the stimulation of muscle hypertrophy - through increased IGF1-AKT1-mTORC1 or reduced myostatin signaling - is associated with glycolysis and a metabolic reprogramming reminiscent to that which occurs in cancer cells [13].

We recently reported that the protein abundance of glycolytic and cancer metabolic reprogramming enzyme pyruvate kinase muscle (PKM; EC 2.7.1.40) isoform 2 (PKM2) increases in human vastus lateralis after 6 weeks of resistance training, and is necessary for basal and IGF-1 stimulated C2C12 myotube growth [25]. Another specific cancer metabolism-associated enzyme that may support muscle hypertrophy is 3-phosphoglycerate dehydrogenase (PHGDH, E.C. 1.1.1.95) [17,26]. PHGDH channels 3-phosphoglycerate out of glycolysis and into serine biosynthesis and one-carbon metabolism, which is crucial for nucleotide and amino acid synthesis, epigenetics, and redox defence [27,28]. The knockdown of PHGDH inhibits proliferation of cancer cells [29], endothelial cells [30], and fibroblasts [31], suggesting that PHGDH-mediated metabolic reprograming is important for proliferation and cellular growth. Muscle stem cells express more *Phgdh* mRNA when they become activated and start to proliferate (supplementary data of [32]). *Phgdh* gene expression also increases in terminally differentiated pig muscles when hypertrophy is stimulated with the β2-agonist ractopamine [33]. Together, this shows that PHGDH becomes activated and/or more abundant in proliferating cells and in at least one model of skeletal muscle hypertrophy.

Currently, it is unclear whether a hypertrophying muscle reprograms its metabolism similar to cancer cells so that glycolytic intermediates can facilitate anabolic reactions, such as serine biosynthesis and one-carbon metabolism. Therefore, the aim of this study was to investigate whether hypertrophying mouse myotubes shunt carbon from glucose into amino acids and nucleotides to support protein and RNA synthesis, respectively. We also investigated whether inhibition of glycolytic flux and manipulation of *Phgdh* expression affected myotube size in untreated or IGF-1-treated myotubes. We found that mouse myotubes indeed convert carbon from glucose into protein and RNA, and that glucose-carbon incorporation into protein increases during IGF-1-induced hypertrophy. Additionally, inhibition of glycolysis and knockdown of *Phgdh* expression attenuates myotube size, whereas overexpression of *PHGDH* increases myotube size. Collectively, these findings suggest that glycolysis is important for hypertrophying mouse myotubes, presumably through the provision of biosynthetic intermediates that support anabolism, reminiscent of proliferating cancer cells.

2. Materials and methods

2.1. Cell culture

2.1.1. C2C12 muscle cells

C2C12 muscle cells (ATCC, Cat#CRL-1772, RRID:CVCL_0188; Middlesex, UK; cells were regularly tested for contamination) were grown to confluency in growth medium containing Dulbecco's Modified Eagle's Medium (DMEM; Gibco, Cat#31885, Waltham, MA, USA), 10 % foetal bovine serum (FBS; Biowest, Cat#S181B, Nuaillé, France), 1 % penicillin/streptomycin (Gibco, Cat#15140, Waltham, MA, USA), and 0.5 % amphotericin B (Gibco, Cat#15290–026, Waltham, MA, USA), and incubated at 37 °C in humidified air with 5 % CO_2. Once ≈90 % confluent, medium was changed to differentiation medium consisting of DMEM supplemented with 2 % horse serum (HyClone, Cat#10407223, Marlborough, MA, USA) and 1 % penicillin/streptomycin. This medium was refreshed daily until treatment.

2.1.2. Primary mouse muscle cells

Primary muscle stem cells were obtained from extensor digitorum longus (EDL) muscles of 6-week to 4-month old mice of a C57BL/6 background. The experiments were conducted with post-mortem material from surplus mice (C57BL/6 J) due to breeding excess, which had to be terminated in the animal facility and therefore did not fall under the Netherlands Law on Animal Research, in agreement with the Directive 2010/63/EU. The EDL muscles were incubated in collagenase type I (Sigma-Aldrich, Cat#C0130, Saint Louis, MO, USA) at 37 °C in air with 5 % CO_2, for 2 h. The muscles were washed in DMEM containing 1 % penicillin/streptomycin and incubated in 5 % bovine serum albumin (BSA)-coated dishes with DMEM for 30 min, at 37 °C in air with 5 % CO_2, to inactivate collagenase. Single muscle fibres were separated by gently blowing with a blunt-ended, sterilized Pasteur pipette. Subsequently, muscle fibres were seeded in a matrigel (VWR, Cat#734–0269, Radnor, PA, USA)-coated 6-well plate containing growth media (DMEM, 1 % penicillin/streptomycin, 10 % horse serum), 30 % FBS, 2.5 ng ml^{-1} recombinant human fibroblast growth factor (Promega, Cat#G5071, Madison, WI, USA), and 1 % chicken embryo extract (Seralab, Cat#CE-650-J, Huissen, The Netherlands). Primary myoblasts were allowed to proliferate and migrate from the muscle fibres for 3–4 days at 37 °C in air with 5 % CO_2. After gentle removal of the muscle fibres, myoblasts were cultured in matrigel-coated flasks until passage 5. Cells were preplated in an uncoated flask for 15 min with each passage to reduce the number of fibroblasts in culture. Cell population was 99 % Pax 7^{+}. All experiments with primary myoblasts were performed on matrigel-coated plates and once confluent myoblasts were cultured in

differentiation medium until treatment.

2.2. Cell compound treatments

2.2.1. Inhibition of mTORC1 via rapamycin

On day 2–3 of differentiation, C2C12 myotubes were incubated in differentiation medium plus one of the following treatments for 48 h: bovine serum albumin (BSA) vehicle control, IGF-1 (100 ng ml^{-1}; recombinant Human IGF-1, Peprotech, Cat#100–11, London, UK), rapamycin (100 ng ml^{-1}; Calbiochem, Cat#553210, Watford, Hertfordshire, UK), and IGF-1 + rapamycin.

2.2.2. Inhibition of glycolysis via 2-deoxyglucose (2DG)

On day 3–4 of differentiation, C2C12 and primary myotubes were treated with differentiation media supplemented with either IGF-1 (100 ng ml^{-1}), 2DG (5 mM, Cat#D6134, Sigma Aldrich), or IGF-1 + 2DG for 24 h.

2.2.3. Inhibition of AKT via compound MK-2206

Differentiation medium was refreshed daily and on day 3-4 C2C12 myotubes were treated with MK-2206 (Bio-Connect, Cat#HY-10358, Netherlands). After a 1-h incubation with MK-2206 (10 μM, 100 μM or 1000 μM), IGF-1 (100 ng ml^{-1}) was added. Cells were harvested after 24 h of IGF-1 treatment.

2.3. Phgdh/PHGDH manipulation

2.3.1. siRNA-mediated silencing of phgdh

For PHGDH loss-of-function experiments, *Phgdh* was silenced in C2C12 and primary myotubes using small interfering RNA (Ambion, Carlsbad, CA, USA, see Table 1 for siRNA sequences). C2C12 myoblasts or primary myoblasts were grown and differentiated as described. On day 2 of differentiation, myotubes were transfected with siRNA targeted against *Phgdh* using the liposome-mediated method (Lipofectamine RNAiMAX, Invitrogen, Cat#13778100, Carlsbad, CA, USA). As a negative control, a non-targeting siRNA sequence (siControl) was used. siRNA was diluted in Opti-MEM reduced serum medium (ThermoFisher, Cat#31985070, Waltham, MA, USA) and incubated for 5–10 min with Lipofectamine mixture. RNA-lipofectamine complexes were added to each well at a final concentration of 20 nM of siRNA. On day 3, the differentiated myotubes were treated with IGF-1 (100 ng ml^{-1}) and harvested on day 4 (≈48 h post-transfection).

2.3.2. PHGDH plasmid cloning, retrovirus, and retroviral transduction

For PHGDH gain-of-function experiments, we subcloned a human PHGDH pMSCV retroviral vector and transduced C2C12 myoblasts prior to differentiation. Human PHGDH cDNA (transcript variant NM_006623.4, which encodes a protein of 533 amino acids) was amplified by RT-PCR and cloned into a pMSCV-IRES-eGFP plasmid using the In-Fusion® HD Cloning Kit (Takara, Cat#638920, Shiga, Japan) following manufacturer instructions (see Table 2 for primer sequences).

For retroviral particle production, HEK293T cells were seeded at a density of 3×10^6 cells per T75 flask 24 h prior to transfection. 1 h before transfection, medium was changed to 7 ml of fresh growth medium (DMEM Glutamax (Gibco, Cat#10566016, Waltham, MA, USA), 10 % FBS), into which the transfection mixture was added. For transfection mixture, 4 μg of PHGDH plasmid or 4 μg of empty vector plasmid (Addgene, plasmid #52107) was combined with 4 μg of DNA RV helper plasmid (Addgene, plasmid #12371) in 1800 μl of Opti-MEM. 6 μl of Lipofectamine Plus reagent was then added and incubated for 5 min at room temperature, followed by 24 μl of Lipofectamine LTX (ThermoFisher, Cat#15338100, Waltham, MA, USA) for a further 30-min incubation at room temperature. Transfection medium was changed to fresh growth media 6 h and 24 h after transfection. 48 h post transfection, medium was changed to 7 ml of fresh growth medium and retroviral particles were collected 12, 24, and 36 h after the last medium change by passing all 7 ml of harvested medium through 0.45 μm filters.

For retroviral infection, 3×10^4 C2C12 cells were seeded in a 6-well plate overnight at 37 °C in a 5 % CO_2 incubator. 1 h prior to infection, medium was changed to 1.5 ml of fresh growth medium and cells were transduced by adding retroviral particles at a ratio of 1:4. Cells were incubated until reaching ≈90 % confluence and then differentiated as described in virus-free medium. Diameter measurements (see section 2.6.2.) of transduced myotubes were performed on days 3 and 4 of differentiation, prior to- and after- 24 h of ±IGF-1 (100 ng ml^{-1}) stimulation, respectively.

Table 1
siRNA information.

Silenced gene	Sense	Anti-sense
Phgdh	CCCGAAUGCAAUCCUUUGGTT	CCAAAGGAUUGCAUUCGGGTG
Control	AGUACUGCUUACGAUACGGTT	CCGUAUCGUAAGCAGUACUTT

Table 2
Primers.

Gene	*PHGDH*
Forward	CGCCGGAATTAGATCTATGGCTTTTGCAAATCTGCG
Reverse	GGAAGGTCAAGGTGAAGATTGAGCTCATATACAATT

2.4. Determination of protein abundance and signal transduction

2.4.1. Protein extraction

Cells were lysed on ice in 500 μl of radioimmunoprecipitation assay (RIPA) buffer (Sigma-Aldrich, R0278, Saint Louis, MO, USA) supplemented with phosphatase (1:250, Sigma-Aldrich, 04,906,837,001, Saint Louis, MO, USA) and proteinase (1:50, Sigma-Aldrich, Cat#11836153001, Saint Louis, MO, USA) inhibitor cocktails, 0.5 M Ethylenediaminetetraacetic acid (EDTA; 1:500), sodium fluoride (NaF; 1:50) and sodium orthovanadate (1:50). Lysates were left on ice for 15 min and cellular debris removed by centrifuging at 13,000 rpm for 15 min at 4 °C. Supernatants were then transferred to fresh eppendorfs and frozen at −80 °C (for radiolabelled glucose to protein) or their protein concentrations calculated (for Western blotting) using a Pierce BCA Protein Assay kit (Thermo Scientific, Cat#23225, Waltham, MA, USA).

2.4.2. SDS-PAGE immunoblotting

Respective volumes of lysate were diluted in 5× Laemmli SDS buffer and denatured for 5 min at 95 °C, prior to immunoblotting. Samples were then electrophoresed on 4-12 % Bis-Tris gels (Bio-Rad, Cat#3450125, Hemel Hempstead, UK) and transferred onto PVDF membranes (GE Healthcare, Cat#15269894, Chicago, IL, USA) using a semi-dry transfer blotter (Bio-Rad). Membranes were blocked in prime blocking agent (GE Healthcare, Cat#RPN418, Chicago, IL, USA), then incubated with primary Phospho-P70S6K (Thr389; 1:2000; Cell Signaling Technology, Cat#9234, Leiden, The Netherlands, RRID: AB_2269803), Phospho-AKT (Ser473, 1:2000; Cell Signaling Technology, Cat#4060, Leiden, The Netherlands, RRID:AB_2315049), α-TUBULIN (1:10,000; Cell Signaling Technology, Cat#2125, Leiden, The Netherlands, RRID:AB_2619646), pan-ACTIN (1:1000, Cell Signaling Technology, Cat#8456, Leiden, The Netherlands, RRID:AB_10998774), PHGDH (1:1000; Cell Signaling Technology, Cat#13428, Leiden, The Netherlands, RRID:AB_2750870), Phospho-AMPK (Thr172, 1:500; Cell Signaling Technology, Cat#2531, Leiden, The Netherlands, RRID:AB_330330), and anti-rabbit/mouse IgG secondary antibody (1:2000; Roche, Cat#12015218001, Basal, Switzerland) prior to fluorescent imaging. Protein bands from blot images were normalized to loading control by densitometric analysis using ImageJ software (http://rsbweb.nih.gov/ij/, National Institutes of Health, Bethesda, MD, USA; RRID:SCR_003070).

2.5. ^{14}C-glucose incorporation analysis

1 μl ml^{-1} of 0.1 mCi ml^{-1} ^{14}C glucose (PerkinElmer, Cat#NEC042-V250UC, Waltham, MA, USA) was added to differentiation medium at the time of C2C12 myotube treatments with vehicle, IGF-1, or IGF-1 + rapamycin compounds (see section 2.2.1).

2.5.1. Gel phosphor-imaging

Protein was extracted, and samples prepared and electrophoresed as described in section 2.4. The 4-12 % Criterion XT pre-cast Bis-Tris gel (Bio-rad, Cat#3450123, Hemel Hempstead, UK) was stained with Silver Stain (Bio-rad, Cat#1610481, Hemel Hempstead, UK) and imaged as a loading control quality check. The gel was then dried using a gel dryer and incubated with an imaging plate, protected from light, inside a radiography cassette. After 48 h the plate was imaged using a phosphor-imager (Fuji FLA3000).

2.5.2. ^{14}C-glucose to protein and RNA flux

Protein was isolated from other macromolecules by acetone precipitation of harvested lysates and the resulting protein pellet was resuspended in phosphate buffered saline (PBS). RNA was extracted using the RNeasy Mini Kit (Qiagen, Cat#74104, Valencia, CA, USA) according to manufacturer's instructions. The elution was then placed in 4 ml of scintillation fluid (Insta-Gel Plus, PerkinElmer) for 24 h (to homogenize samples) before measuring radioactivity of the samples in a scintillation counter. Results for protein and RNA are presented in counts per minute (CPM) per 10 cm diameter Petri dish (growth surface area ≈55 cm^2).

2.6. Myotube size measurement

2.6.1. Immunocytochemistry

C2C12 myoblasts were seeded in chamber slides coated with extracellular matrix gel (E6909; Sigma-Aldrich, St. Louis, MO, USA), then differentiated and treated as described in sections 2.1.1. and 2.2.1, respectively. Chamber slides were fixed with 4 % paraformaldehyde in PBS for 10 min at room temperature, washed 3 times in PBS, and then permeabilized for 6 min with 0.5 % Triton X-100 in PBS. Cells were washed 3 more times in PBS, blocked for 30 min in blocking buffer (20 % goat serum in PBS; Dako, Ely, UK), and incubated with anti-myosin heavy chain primary antibody (1:400; MF20 IgG2b), diluted in 0.025 % Tween 20 in PBS, overnight with gentle rocking at 4 °C. Cells were then washed 3 times in 0.025 % Tween 20 in PBS, and incubated with anti-mouse secondary antibody (1:500; Licor, Cambridge, UK) in 0.025 % Tween 20 in PBS, for 90 min at room temperature with gentle rocking. Slides were counterstained with ProLong Gold antifade reagent with DAPI (Invitrogen, Paisley, UK), then fluorescently imaged on an Axioscan. Z1 slide scanner (Zeiss, Cambridge, UK). Images from 3 random fields of view were taken per chamber at 5× magnification. This was repeated for 3 biological replicates, giving a total of 9 images per treatment. Images were exported into ImageJ software and blinded measurements were taken according to methods modified from Trendelenburg et al. (2009) [34]: 5–10 myotubes were measured per image and the average size of each myotube was calculated as the mean of 3 diametric measurements taken at equidistant intervals along its length. The average myotube diameter of the 5 largest myotubes per biological replicate (n = 3) per condition was used for statistical analysis.

2.6.2. Light microscopy

Four images were taken per well at 10× magnification after 24 h of either 2DG ± IGF-1 (section 2.2.2.), MK-2206 ± IGF-1 (section 2.2.3.), or PHGDH silencing/overexpression ± IGF-1 (section 2.3) treatment. Diameters were measured in 20–50 myotubes per biological replicate at 3 equidistant locations along the length of the cell using ImageJ, taking into consideration the pixel-to-aspect ratio.

2.7. Lactate concentration

Cultured medium was directly removed of lactate dehydrogenase using a 10 kDa molecular weight cut-off spin filter. Lactate was subsequently measured in 0.5 μl of filtrate and assayed in duplicate in a 96 well plate using the Lactate Assay Kit (Sigma-Aldrich, Cat#MAK064, Saint Louis, MO, USA) according to manufacturer's instructions. Colorimetric absorbance was measured at 570 nm and lactate concentrations were determined against the standard curve.

2.8. Gene expression

2.8.1. RNA isolation

After washing cells with PBS, cells were lysed in TRI reagent (Invitrogen, 11,312,940, Carlsbad, CA, USA) and stored at −80 °C. RNA was isolated using RiboPureTMkit (Applied Biosystems, Foster City, CA, USA), and concentration and purity determined by NanoDrop spectrophotometry. RNA was converted to cDNA with high-capacity RNA-to-cDNA master mix (Applied Biosystems, Foster City, CA, USA). cDNA was diluted 10× and stored at −20 °C.

2.8.2. Real-time quantitative PCR

Gene expression was assessed by real-time quantitative PCR (see Table 3 for primer details) using fluorescent SYBR Green Master Mix (Fischer Scientific, Cat#10556555, Pittsburgh, PA, USA). Reactions were run in duplicate and referenced to the 18 S ribosomal RNA (rRNA) housekeeping gene. Relative changes in gene expression were determined by the ΔΔCt method.

2.9. Statistical analysis

The Shapiro–Wilk test was used to assess normality. Normally distributed data were analysed as appropriate using: ratio paired *t*-test, repeated measures one-way analysis of variance (ANOVA), or a repeated measures two-way ANOVA/mixed-effects model with Šidák correction. When assumptions of a two-way ANOVA were not met, data were transformed using Tukey's Ladder of Powers (rcompanion). If assumptions were still not met, or for one-factor comparisons of non-normally distributed data, a Friedman's or (in the case of missing values) Kruskal-Wallis test was used with Dunn's multiple comparisons. The statistical method used, as well as main and interaction effects, are included in figure legends. Post-hoc analyses were only performed if main or interaction effects passed a threshold of $p < 0.05$, and significant comparisons are presented in figures by stars (*); however, exact p-values for $p \leq 0.1$ are also reported. In the results section, changes discussed are significant (i.e. main, interaction, or post-hoc effect) unless stated otherwise. Normal data are presented as bar plots with mean ± SD and individual data points, whereas nonparametric data are visualized using box and whisker plots with Tukey distribution and individual data points (except for Fig. 6d, as described in the figure legend). Statistical analyses were performed using Prism 9.4.0 (GraphPad Prism, RRID:SCR_002798) and R 4.1.2 (www.r-project.org).

Table 3
qPCR primers.

Gene	Forward	Reverse
18S rRNA	GTAACCCGTTGAACCCCATT	CCATCCAATCGGTAGTAGCG
Phgdh	CCCACTATGATTGGCCTCCT	AGACACCATGGAGGTTTGGT
Trim63 (*MuRF1*)	GGGCTACCTTCCTCTCAAGTGC	CGTCCAGAGCGTGTCTCACTC
Fbxo32 (*MAFbx*)	AGACTGGACTTCTCGACTGC	TCAGCTCCAACAGCCTTACT

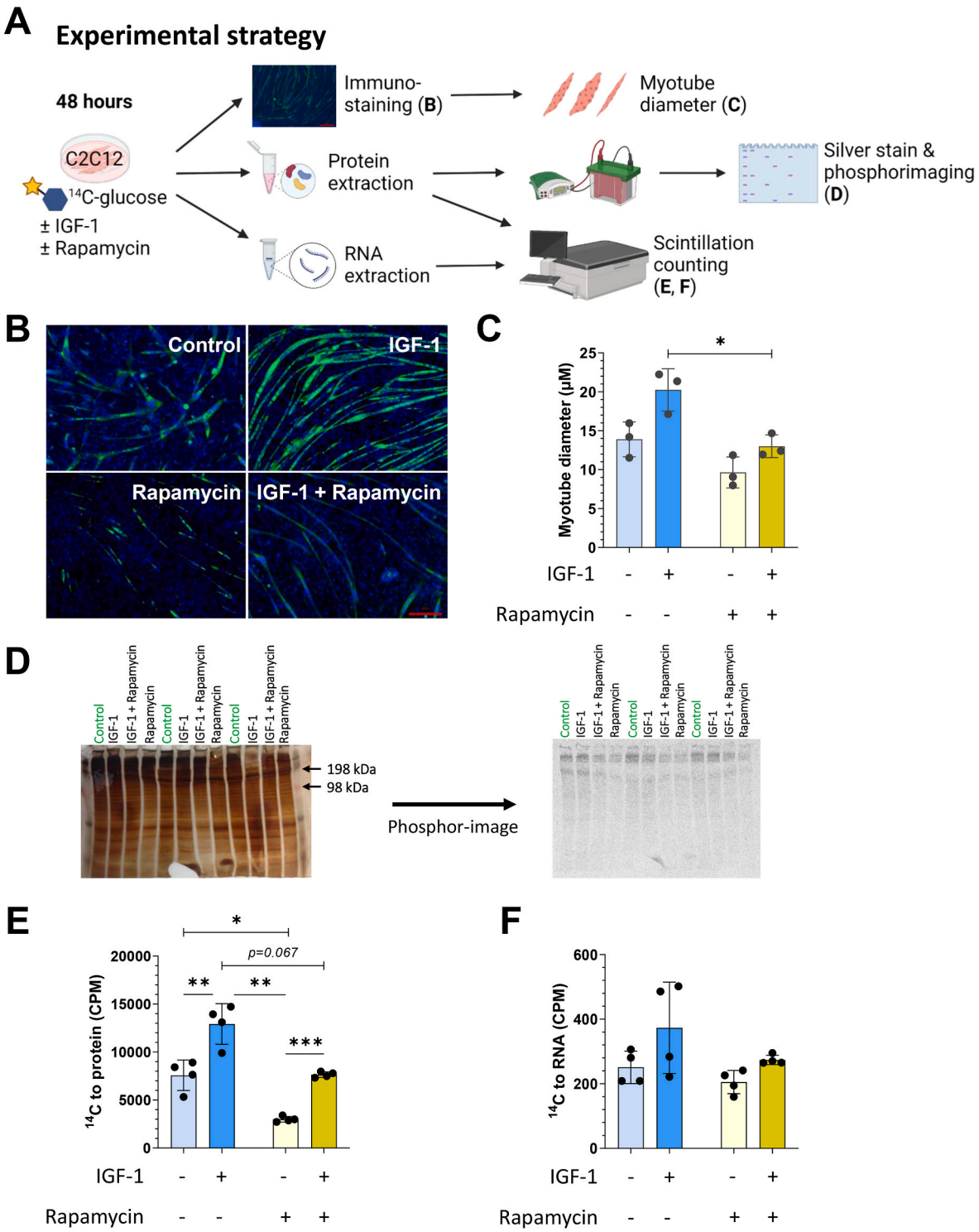

Fig. 1. Glucose-derived (^{14}C) carbon can be converted into protein and RNA, particularly in IGF-1-stimulated C2C12 myotubes, suggesting cancer-like metabolic reprogramming so that energy metabolites are channelled into anabolic pathways. (a) Schematic depiction of the experimental strategy. (b) Representative images and (c) quantification of myotube diameter after IGF-1 and/or rapamycin treatment (IGF-1 effect, p = 0.089; Rapamycin effect, p = 0.017) (n = 3). Scale bar is 200 μm. (d) Dried gel showing all protein bands and radioactivity detected in the gel using a phosphor-imager (n = 3 on a single gel). The phosphor-image provides visual confirmation that radioactivity was detectable in protein but was not quantified. (e, f) Radioactivity (n = 4, in counts per minute; CPM) per 10 cm dish in (e) precipitated protein lysates (IGF-1 effect, p < 0.0001; Rapamycin effect, p = 0.006; interaction, p = 0.001) and (f) extracted RNA (IGF-1 effect, p = 0.07). *Significantly different between indicated conditions, repeated measures two-way ANOVA with Šidák correction (*p < 0.05, **p < 0.01, and ***p < 0.001).

3. Results

3.1. IGF-1 induced myotube growth increases ^{14}C-incorporation into protein and RNA

A key feature of metabolic reprogramming in cancer is increased glucose uptake and a greater shunting of glucose-derived glycolytic intermediates, and other metabolites, from energy metabolism into anabolic pathways [13]. In relation to skeletal muscle hypertrophy, a key question is: does a similar shunting of glucose-derived metabolites occur in hypertrophying muscles? To try to answer this question, we stimulated growth of C2C12 myotubes with 100 ng ml^{-1} of IGF-1 [35] ± 100 ng ml^{-1} of the mTORC1 inhibitor rapamycin for 48 h and measured the rate at which ^{14}C derived from ^{14}C-glucose was incorporated into protein and RNA (Fig. 1a).

These experiments revealed that ^{14}C-incorporation into both protein and RNA was already measurable at baseline (Fig. 1d–f). IGF-1 tended to increase myotube diameter by ≈50 ± 39 % (IGF-1 effect, *p=0.089*) (Fig. 1b and c) and ^{14}C-incorporation into protein by ≈72 ± 10 %, versus control (Fig. 1e). Additional treatment with rapamycin attenuated IGF-1-stimulated myotube growth and reduced ^{14}C incorporation into protein by ≈59 ± 10 % compared to control, and ≈76 ± 4 % to ≈39 ± 12 % versus IGF-1 and IGF-1 + rapamycin stimulation, respectively (Fig. 1e). This suggests that ^{14}C incorporation into protein is somewhat mTORC1-dependent. Nevertheless, ^{14}C detection was still ≈156 ± 17 % higher in IGF-1 + rapamycin conditions versus rapamycin alone, consistent with mTORC1-independent protein synthesis [36] and the complimentary role of rapamycin-insensitive pathways during muscle hypertrophy [37]. Generally, little ^{14}C was incorporated into RNA (IGF-1 effect, p = 0.07; Fig. 1f).

Together this data indicates that C2C12 myotube growth is associated with a presumed increase in 'glucose → glycolytic intermediates → non-essential amino acid(s) → protein' series of reactions. However, the possibility of detecting protein glycosylation cannot be ruled out in the current experimental design.

3.2. Blocking glycolysis attenuates myotube growth

Glycolysis is not only a key metabolic pathway but also a feeder pathway for anabolic reactions [13]. We therefore tested whether inhibition of glycolysis affected C2C12 and primary mouse myotube size and growth. For this purpose, we inhibited glycolysis for 24 h with

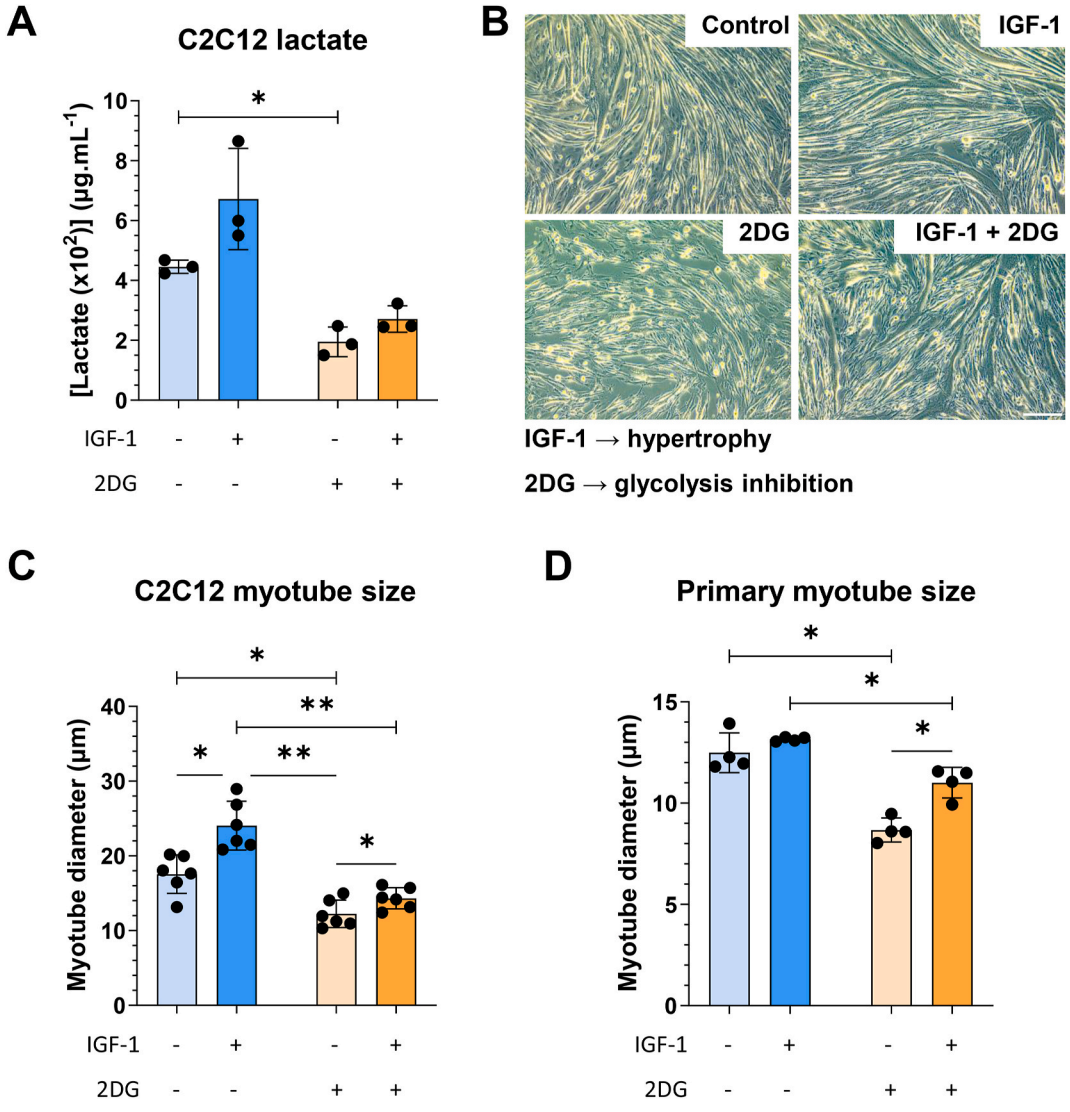

Fig. 2. Glycolysis inhibition attenuates C2C12 and primary myotube growth. Effects of 2DG and IGF-1 on (a) lactate concentrations (IGF-1 effect, p = 0.01; 2DG effect, p = 0.031) (n = 3), (b, c) C2C12 myotube diameter (IGF-1 effect, p = 0.0004; 2DG effect, p = 0.0008; interaction, p = 0.022) (n = 5) and (d) primary myotube diameter (IGF-1 effect, p = 0.005; 2DG effect, p = 0.002) (n = 4). Scale bar is 200 µm *Significantly different between indicated conditions, repeated measures two-way ANOVA with Šidák correction (*p < 0.05 and **p < 0.01).

2-deoxy-D-glucose (2DG) [38], and measured the diameter of control and IGF-1 stimulated myotubes. In C2C12, we found that 2DG treatment reduced lactate concentrations as expected (Fig. 2a) (2DG effect, $p = 0.031$), and attenuated myotube growth in non-treated (≈30 ± 10 %) and IGF-1-treated (≈49 ± 7 %) myotubes (Fig. 2b and c).

In primary muscle cells, despite an overall effect of IGF-1 ($p = 0.005$), the impact of IGF-1 on myotube growth was less apparent than in C2C12 (6 ± 7 % versus 38 ± 20 %). Still, consistent with effects in C2C12 the addition of 2DG also blunted primary myotube diameter by ≈30 ± 7 % and ≈16 ± 5 % under basal and IGF-1 conditions, respectively (Fig. 2d). Both C2C12 and primary myotubes showed an IGF-1-induced growth response under 2DG conditions (Fig. 2c and d); although, the magnitude of myotube growth was reduced by 2DG in C2C12 cultures (≈38 ± 19 % versus ≈18 ± 10 %; IGF-1 x 2DG interaction, $p = 0.022$) (Fig. 2c). Collectively, these data suggest that inhibition of glycolytic flux impairs basal myotube size and may also be rate-limiting for IGF-1-stimulated growth.

3.3. Glycolysis inhibition and IGF-1 affect regulators of protein turnover and PHGDH

The inhibition of glycolytic flux through 2DG may not only affect the generation of glycolytic intermediates for anabolic reactions but also energy-sensitive signaling mechanisms, such as activation of AMP-activated protein kinase (AMPK), which could have contributed to the observed attenuation of myotube growth. Under conditions of nutrient stress, rising ADP and/or AMP levels displace ATP binding at regulatory sites in AMPK subunits, leading to Thr172 phosphorylation (by upstream kinase LKB1) and increased AMPK enzymatic activity [39]. Once active, AMPK can suppress mTORC1-dependent protein synthesis [39–42], and promote myofibrillar catabolism through FOXO-mediated upregulation of the E3-ubiquitin ligases MAFbx (*Fbxo32*) and MURF1 (*Trim63*) [41]. Conversely, FOXO transcription factors are negatively regulated by IGF-1 [43].

We observed the expected decrease of AMPK phosphorylation (Fig. 3a, c) and E3-ligase mRNA (Fig. 3d and e) in C2C12 myotubes under IGF-1 conditions. Alternatively, there was no evidence of increased AMPK activation (Fig. 3a, c) or *Fbxo32* and *Trim63* gene expression (Fig. 3d and e) with 2DG treatment, indicating that a diminished energy state did not attenuate myotube size through AMPK. mTORC1 can also be inhibited via AMPK-independent mechanisms in response to glucose starvation [42]. Consistent with this, 2DG decreased phosphorylation of key mTORC1 substrate P70S6K compared to IGF-1 stimulation (Fig. 3b and c), suggesting modest reduction of basal mTORC1 signaling when glycolysis was attenuated. However, 2DG had no apparent effect on phospho-P70S6K under IGF-1 conditions (Fig. 3b and c). These data suggest that the 2DG-associated impairment of myotube size may stem from inhibition of mTORC1-dependent myofibrillar protein synthesis at baseline; whereas availability of glycolytic intermediates for anabolic reactions, as opposed to mTORC1 activity per se, may be rate-limiting under IGF-1-treated/growth-stimulated conditions, at least in C2C12 (Fig. 2c). Albeit, this latter effect was not sufficient to completely prevent myotube growth in response to IGF-1 + 2DG (Fig. 2c and d).

3.4. Silencing of PHGDH attenuates myotube growth

To address the potential importance of glycolysis-derived biosynthetic precursors, we next studied the role of cancer reprogramming-associated enzyme PHGDH. PHGDH catalyses the first reaction of the serine biosynthesis pathway (3-phosphoglycerate + NAD^+ → 3-phosphooxypyruvate + H^+ + NADH) and is important for one-carbon metabolism [27]. PHGDH limits cell proliferation [29] but may also play a role in post-mitotic growth. Indeed, PHGDH and other serine biosynthesis enzymes are upregulated when stimulating muscle hypertrophy in pigs with the β2-agonist ractopamine [33]. In agreement, we observed that C2C12 myotubes increased *Phgdh* mRNA (≈219 ± 70 %) and protein (≈90 %, interquartile range [IQR] 60–293 %) expression upon IGF-1 stimulation (Fig. 3f–h). However, after lipofectamine-mediated siRNA transfection the effect of IGF-1 on *Phgdh* mRNA was not reproduced in negative control (siControl) C2C12 myotubes (Fig. 4a) and *Phgdh* was only modestly upregulated in siControl primary myotubes (≈9 ± 3 %; adjusted post-hoc, $p = 0.331$) (Fig. 4f). As the process of transfection can substantially alter the transcriptome independently from the cargo being delivered [44], future studies should look to confirm our findings of IGF-1 induced PHGDH expression under native conditions.

To investigate whether normal levels of PHGDH limit myotube size and growth-response, we knocked-down PHGDH through siRNA silencing of mRNA and determined the effect on myotube diameter. In C2C12, siRNA interference reduced *Phgdh* mRNA to ≈31–37 % of baseline levels (Fig. 4a) and PHGDH protein to ≈18–27 % of baseline (Fig. 4b and c). Knockdown of PHGDH decreased average C2C12 myotube size in control and IGF-1-treated cells by ≈30 ± 4 % and ≈51 ± 8 %, respectively (Fig. 4d and e). Consistently, PHGDH silencing (by 52–54 %) (Fig. 4f) also impaired primary myotube growth by ≈25 ± 8 % and ≈35 ± 8 % under the same conditions (Fig. 4g). In contrast to 2DG (Fig. 2c and d), silencing of PHGDH also blocked the effect of IGF-1 in both C2C12 (Fig. 4e) and primary (Fig. 4g) myotubes, implying that PHGDH is necessary for both maintenance of basal myotubes size and IGF-1-mediated growth.

3.5. PHGDH overexpression increases myotube growth

Because PHGDH silencing reduced myotube growth, we then investigated whether a gain of PHGDH is sufficient to increase C2C12 myotube diameter. Overexpression of human PHGDH ($PHGDH^{OE}$) by ≈10 ± 8-fold (Fig. 5a) tended to increase myotube growth (Fig. 5b). Compared to empty vector control (EV), the diameter of $PHGDH^{OE}$ myotubes was ≈19 ± 14 % greater at timepoint 1 (control) ($PHGDH^{OE}$ effect, $p = 0.061$) and ≈11 ± 8 % greater 24 h later ($PHGDH^{OE}$ effect, $p = 0.032$) (Fig. 5c). The size of $PHGDH^{OE}$ myotubes was further augmented (≈27 ± 17 %) by IGF-1 (adjusted post-hoc, $p = 0.089$), although no interaction was detected ($PHGDH^{OE}$ x IGF-1, $p = 0.374$) (Fig. 5c). Together, these results indicate that silencing PHGDH attenuates- whereas PHGDH overexpression increases-myotube size, suggesting that PHGDH is a regulator of skeletal muscle mass.

3.6. AKT regulates PHGDH in C2C12 myotubes

Activation of AKT stimulates aerobic glycolysis (i.e. the Warburg effect) in cancer cells [21], promotes muscle hypertrophy [45], and is associated with a shift towards glycolysis [22]. Therefore, we assessed whether AKT also regulates PHGDH. To study this, we used IGF-1 and MK-2206 to activate and repress AKT, respectively. The highest dose of MK-2206 treatment (1000 μM) tended to reduce activity-associated AKT phosphorylation when compared to IGF-1 stimulation (Fig. 6a), as well as P70S6K phosphorylation – although the effect on P70S6K did not reach statistical significance (one-way ANOVA, $p = 0.092$) (Fig. 6b). 1000 μM of MK-2206 also decreased PHGDH protein abundance by ≈43 ± 20 % versus IGF-1-treatment alone (Fig. 6c and d). Interestingly, this inhibition of AKT and PHGDH at 1000 μM of MK-2206 was coincident with (≈36–38 %) smaller C2C12 myotube diameter compared to IGF-1 treated conditions (Fig. 6e and f). These findings imply that AKT regulates PHGDH, providing a possible mechanism through which metabolism is altered in growing muscle to facilitate anabolism.

4. Discussion

This study reports five findings that support the idea that hypertrophying muscles reprogram their metabolism to support anabolism and growth, reminiscent of cancer cells (Fig. 7). First, the stimulation of

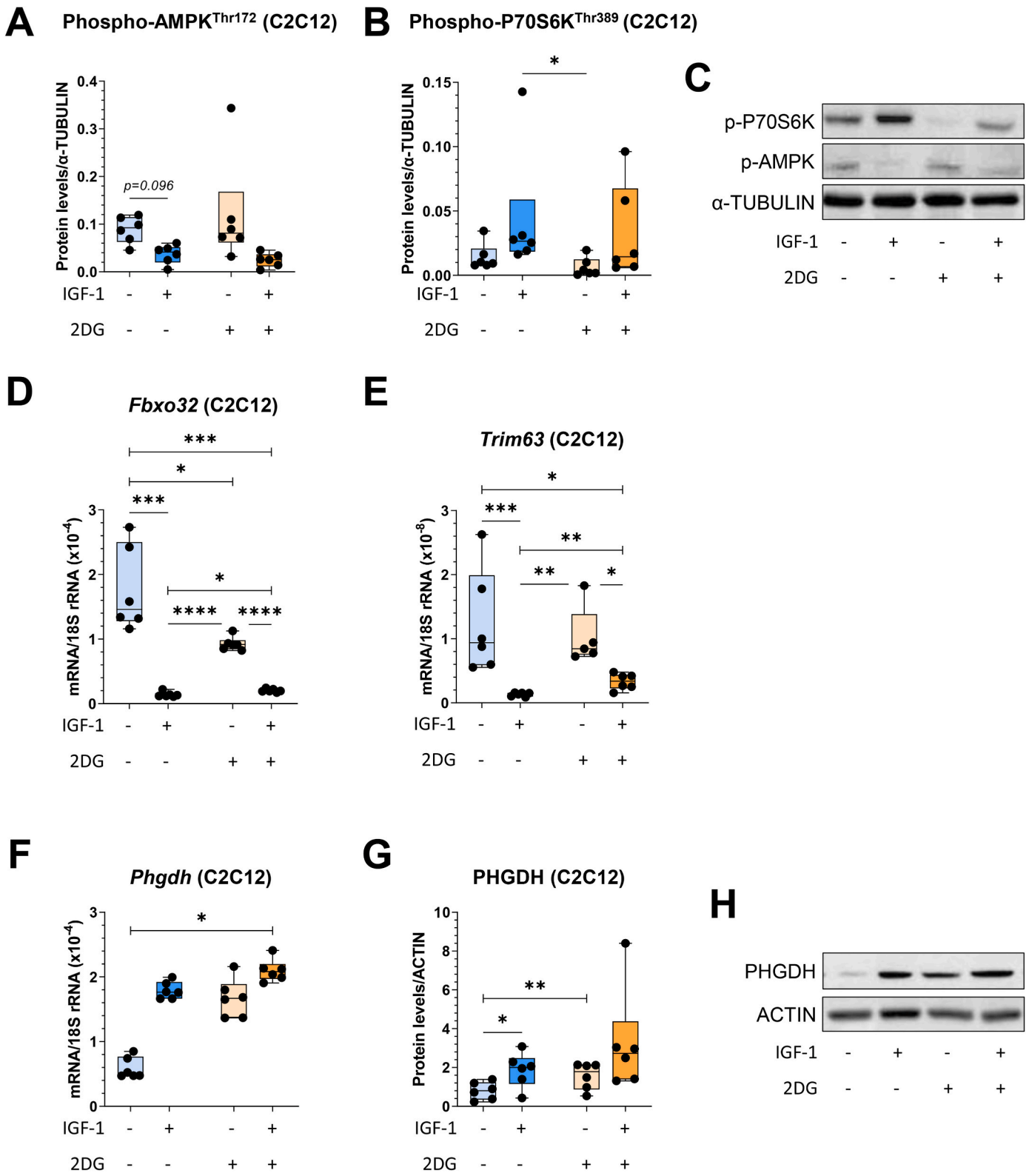

Fig. 3. 2DG effects on protein abundance and mRNA expression in C2C12 myotubes. Effects of 2DG and IGF-1 on (a) phospho-AMPK at residue Thr172 (IGF-1 effect, $p = 0.038$) and (b) phospho-P70S6K at residue Thr389 (Friedman test, $p = 0.01$) ($n = 6$). (c) Representative western blots for phospho-AMPK and phospho-P70S6K, with α-TUBULIN as loading control. (d) Impact of compound treatment on *Fbxo32* (*MAFbx*) (IGF-1 effect, $p < 0.0001$; 2DG effect, $p = 0.065$; interaction, $p = 0.001$) and (e) *Trim63* (*MuRF1*) gene expression (IGF-1 effect, $p < 0.0001$; IGF-1 x 2DG interaction, $p = 0.021$) ($n = 5$–6). (f) IGF-1 and 2DG effects on *Phgdh* mRNA (Friedman test, $p = 0.0002$) and (g, h) protein abundance (IGF-1 effect, $p = 0.028$; 2DG effect, $p = 0.013$) in C2C12 ($n = 6$). *Significantly different between indicated conditions; repeated measures two-way ANOVA or mixed-effects model with Šidák correction; or Friedman test with Dunn's multiple comparisons (*$p < 0.05$, **$p < 0.01$, ***$p < 0.001$, and ****$p < 0.0001$).

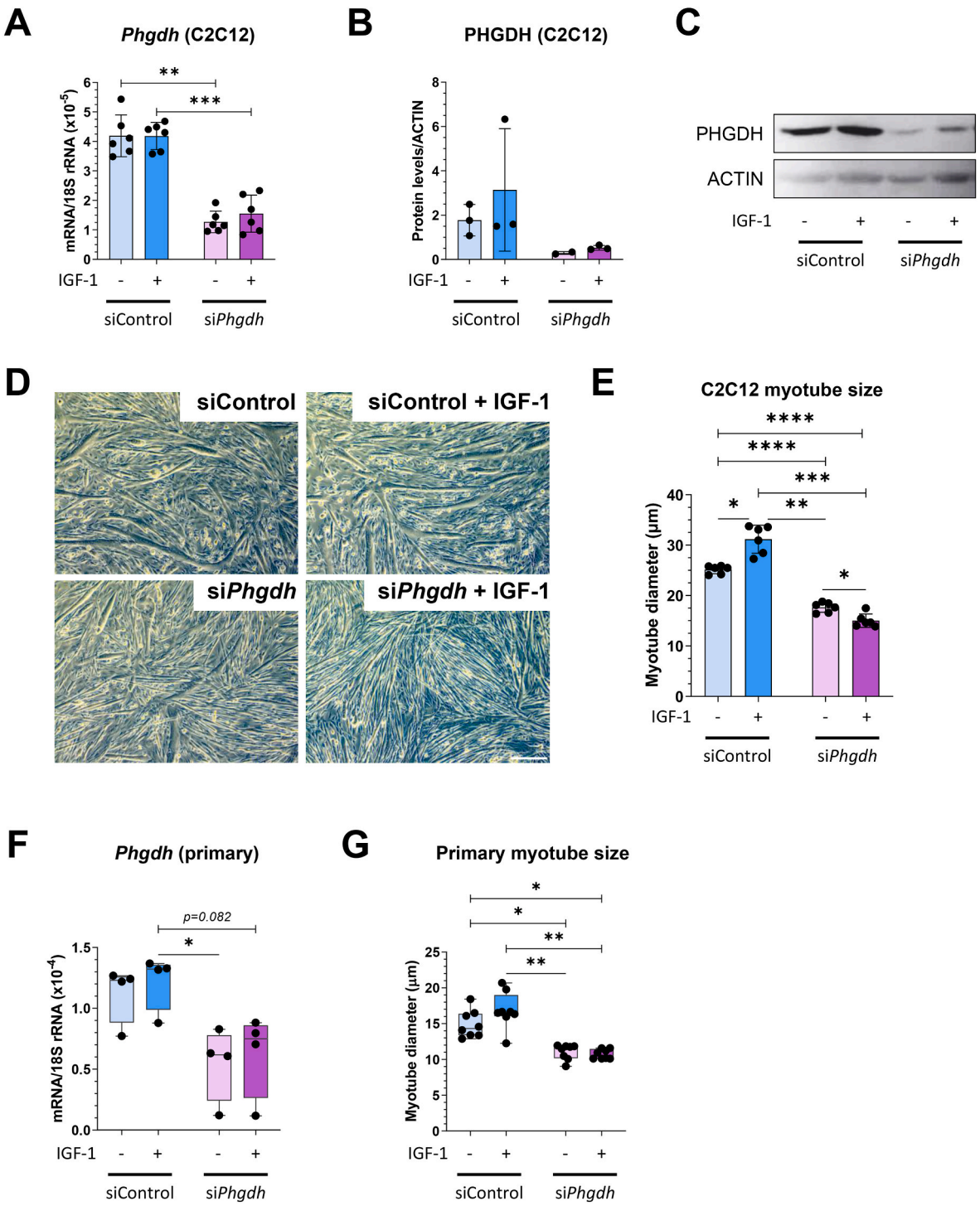

Fig. 4. PHGDH silencing **by siRNA attenuates myotube growth in control and IGF-1-stimulated myotubes.** (a) *Phgdh* mRNA (si*Phgdh* effect, $p = 0.0004$) ($n = 6$) and (b, c) PHGDH protein (si*Phgdh* effect, $p = 0.032$) ($n = 2–3$) levels after siRNA treatment. (d) Morphology of C2C12 myotubes and (e) the impact of PHGDH knockdown on C2C12 myotube diameter (IGF-1 effect, $p = 0.04$; si*Phgdh* effect, $p < 0.0001$; interaction, $p = 0.001$) ($n = 6$). Scale bar is 200 µm. (f) Efficiency of *Phgdh* silencing (Friedman test, $p = 0.0009$) ($n = 4$) and (g) effect on myotube size (Friedman test, $p = 0.0002$) ($n = 8$) in primary mouse myotubes. *Significantly different between indicated conditions; repeated measures two-way ANOVA or mixed-effects model with Šidák correction; or Friedman test with Dunn's multiple comparisons (*$p < 0.05$, **$p < 0.01$, ***$p < 0.001$, and ****$p < 0.0001$).

C2C12 myotube growth, through IGF-1, increases shunting of carbon from glucose into protein synthesis. Second, we confirm that IGF-1 increases glycolytic flux in C2C12 myotubes [20] and report that attenuating glycolytic flux, through 2DG-mediated inhibition, attenuates C2C12 and primary mouse myotube size. Third, silencing of the serine biosynthesis-catalysing enzyme *Phgdh* inhibited C2C12 and primary myotube growth. Fourth, the overexpression of *PHGDH* in C2C12 increases myotube diameter, collectively suggesting that PHGDH regulates normal myotube size and myotube growth. Fifth, the muscle hypertrophy-promoting kinase AKT regulates the expression of PHGDH.

The first conceptual advance of this study is that glucose is not just a substrate for energy metabolism - it also contributes to cell mass as a

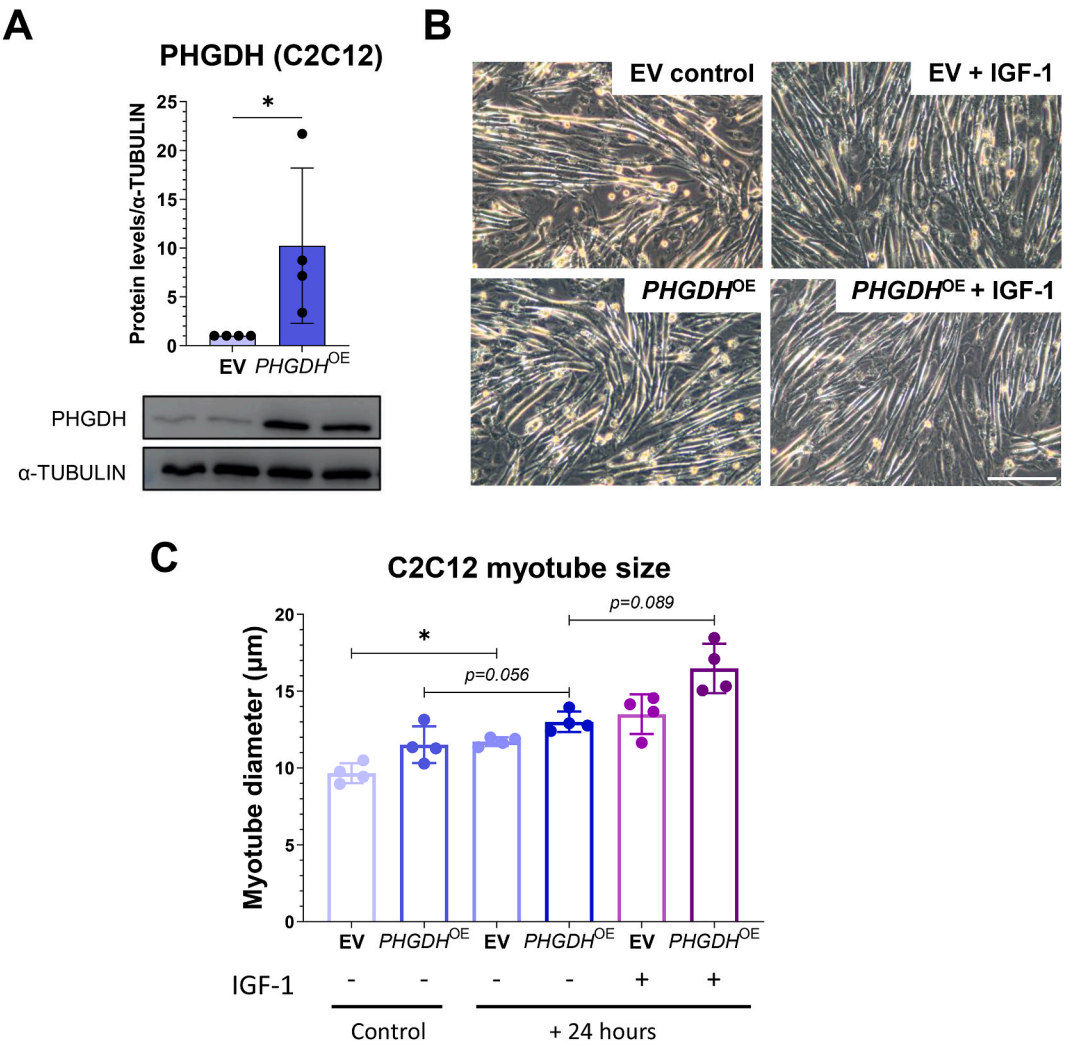

Fig. 5. Overexpression of PHGDH (*PHGDH*^{OE}) in C2C12 increases PHGDH protein levels and myotube size. (a) PHGDH protein abundance after overexpression of human *PHGDH* in C2C12 myotubes (n = 4). Ratio paired *t*-test. Note that we could not distinguish between endogenous mouse PHGDH and overexpressed human PHGDH. (b, c) C2C12 myotube size upon PHGDH overexpression compared to empty vector (EV). Control = untreated cells prior to- and +24 hours = vehicle or IGF-1-stimulated cells after 24 h of exposure (n = 4). Scale bar is 200 μm. Overexpression x time analysis: *PHGDH*^{OE} effect, p = 0.061; Time effect, p = 0.017; interaction, p = 0.08. Overexpression x IGF-1 analysis: *PHGDH*^{OE} effect, p = 0.032; IGF-1 effect, p = 0.008. *Significantly different between indicated conditions, repeated measures two-way ANOVA with Šidák correction (*p < 0.05).

substrate for anabolic reactions, both in proliferating C2C12 myoblasts [46] and in post-mitotic growing myotubes (Fig. 1). Specifically, we found that carbon derived from glucose can be incorporated especially into protein, presumably via a glucose → glycolytic intermediates → amino acid(s) → protein sequence of reactions. This echoes results reported by Hosios et al. showing that 6 % of the total carbon in C2C12 myotubes was derived from glucose over 14 days [46]. Non-essential amino acids are indeed synthesized by human tissues, including skeletal muscle [47], but the regulation of this process is incompletely understood. Furthermore, non-essential amino acids may be required to sustain muscle protein synthesis above fasting levels in the ≥3-5-h post-exercise recovery period [48]; however, it is unclear whether the rate of non-essential amino acid synthesis increases and limits skeletal muscle hypertrophy. The conversion of glucose into biomass may also contribute to the lasting effects on glucose uptake after resistance exercise [18,19] and might further explain the benefits of resistance training for metabolic health [49].

The second finding of this study is that the inhibition of glycolysis blunts C2C12 and primary myotube diameter (Fig. 2), revealing an association between glycolysis and muscle size. A link between glycolytic flux and growth was first demonstrated by Otto Warburg, who showed that sarcomas (i.e. fast-growing tissues) consumed more glucose and synthesized more lactate than normal organs in rats [14]. In mouse muscle, the stimulation of hypertrophy – through IGF-1 in vitro [20] or via gain of *Akt1* [22] or loss of myostatin (*Mstn*) [24] in vivo – not only results in skeletal muscle growth but also increases glycolytic capacity of the hypertrophying muscles. So far there is little data to show whether increased glycolytic flux limits muscle size. However, consistent with our findings (Fig. 2), the deletion of glycolytic enzymes results in smaller muscle fibres in both flies [50] and C2C12 [25].

In addition to reducing the supply of glycolytic intermediates as substrates for anabolic reactions, inhibition of glycolysis could affect the signaling of energy-sensitive molecules, such as AMPK [39], and increase the expression of E3 ubiquitin ligases [41,51]. We did not find any effect of the glycolysis inhibitor 2DG on activity-related AMPK phosphorylation or E3-ligase gene expression (Fig. 3). Instead, smaller myotube size after 24 h of glycolysis inhibition (Fig. 2c and d) may result from attenuated basal rates of protein synthesis. Mechanistically, under low-glucose conditions the glycolytic enzyme GAPDH prevents Rheb from binding mTORC1, thereby inhibiting mTORC1 signaling and protein synthesis [52]. Indeed, 2DG tended to decrease resting phospho-P70S6K levels, but did not impair IGF-1-induced P70S6K

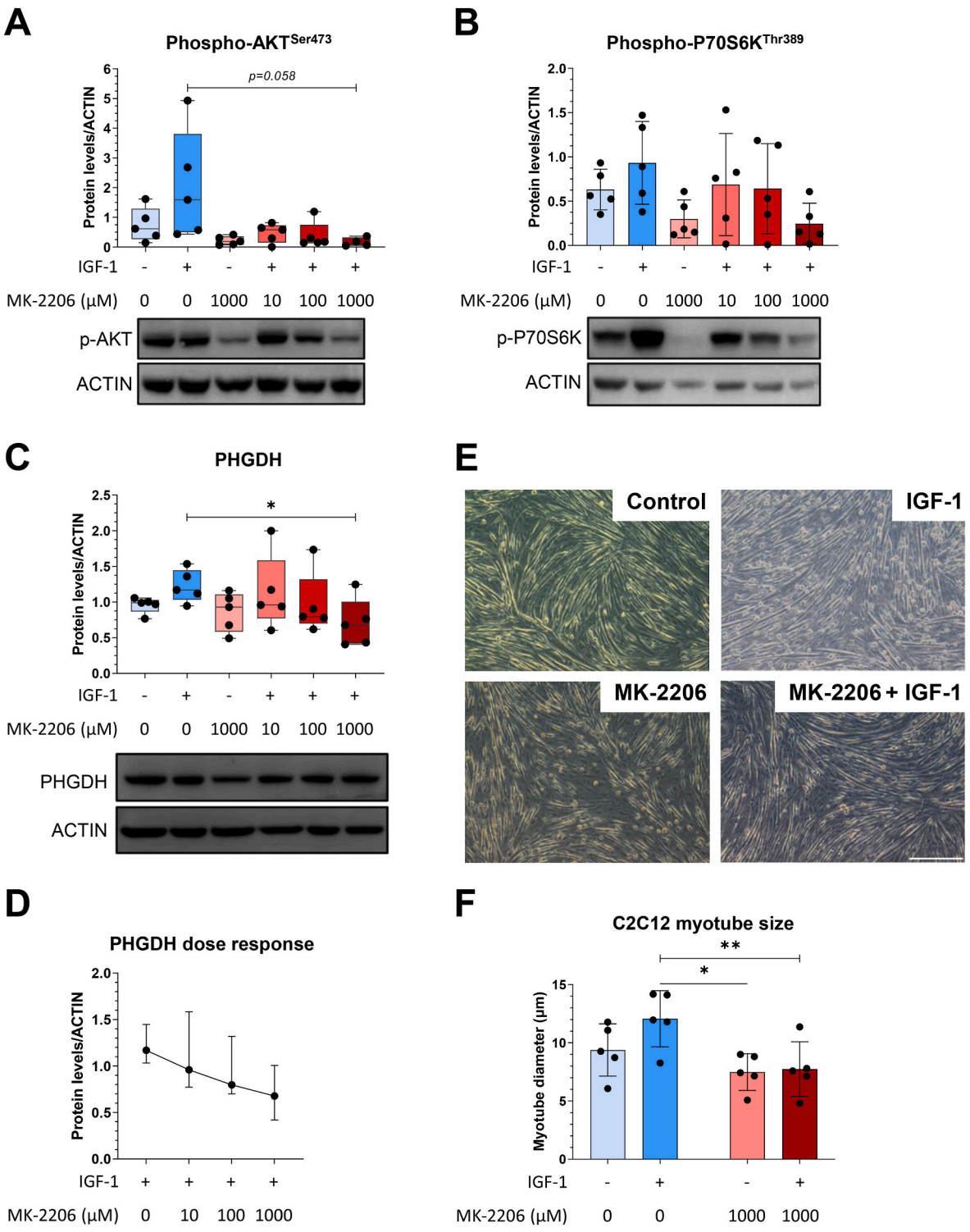

Fig. 6. Blocking AKT in C2C12 myotubes prevents IGF-1 induced PHGDH upregulation. Effect of the AKT inhibitor MK-2206 on (a) phospho-AKT Ser473 (Kruskal-Wallis test, $p = 0.036$) ($n = 4$–5) and (b) phospho-P70S6K Thr389 (repeated measures one-way ANOVA, $p = 0.092$) ($n = 5$) in untreated and IGF-1 treated myotubes. (c) Impact of MK-2206 dose on PHGDH protein abundance (Friedman test, $p = 0.025$), (d) specifically in IGF-1 treated myotubes (Friedman test, $p = 0.006$) ($n = 5$). For (d), dots represent median and error bars depict interquartile range. (e) Representative images and (f) quantification of MK-2206 treatment (1000 μM) on C2C12 myotube diameter (Friedman test, $p = 0.0001$) ($n = 5$). Scale bar is 200 μm. *Significantly different between indicated conditions; Kruskal-Wallis or Friedman test with Dunn's multiple comparisons (*$p < 0.05$ and **$p < 0.01$).

phosphorylation (Fig. 3b and c). Conceivably, IGF-1-stimulated growth may instead be limited by reduced availability of glycolytic intermediates for macromolecular biosynthesis when glycolysis is blunted by 2DG (Fig. 2b and c).

Related to the association between glycolytic flux and muscle hypertrophy, it is worth noting that glycolytic type 2 fibers typically hypertrophy more after resistance training than less glycolytic type 1 fibers [53,54]. This is true even though type 1 fibers have a higher capacity for protein synthesis than type 2 fibers [55]. Future studies should investigate whether the greater hypertrophic potential of type 2 fibers is

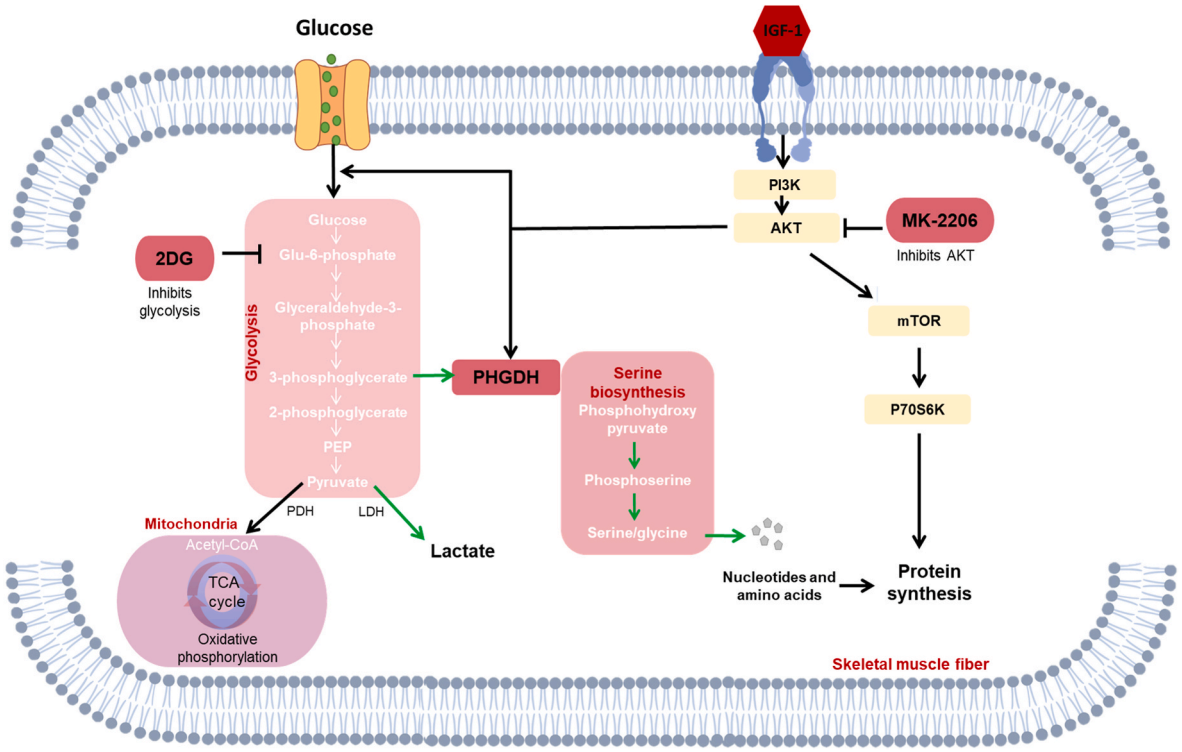

Fig. 7. Schematic showing how PHGDH is involved in IGF-1-induced myotube hypertrophy. Glucose is taken up by muscle cells and, via several glycolytic intermediates, catalysed to pyruvate for energy production in mitochondria. Alternatively, cancer-like metabolic remodelling shunts the glycolytic intermediate 3-phosphoglycerate (3PG) into the de novo serine synthesis pathway. Phosphoglycerate dehydrogenase (PHGDH) catalyses the first step of 3PG to 3-phosphohydroxypyruvate, which is then converted into 3-phosphoserine and, ultimately, serine. Serine is subsequently used for protein synthesis or as a precursor for nucleotide synthesis. IGF-1 induces hypertrophy in post-mitotic muscle cells, which is abolished by 2DG administration or siRNA against PHGDH. AKT stimulates glycolysis and promotes hypertrophy through phosphorylation of P70S6K, thereby increasing protein synthesis. Blocking AKT with compound MK-2206 decreases PHGDH abundance and impairs P70S6K phosphorylation, which leads to reduced myotube size. Dark red indicates where experimental manipulations were applied in this study. Green arrows denote the pathway by which glucose and PHGDH can contribute to muscle size. 2DG, 2-deoxyglucose; MK-2206, AKT inhibitor.

at least in part because these fibers can provide more glycolytic intermediates as substrates for anabolic reactions.

The third and fourth findings are that a loss (Fig. 4) or gain-of-function (Fig. 5) of PHGDH decreases and increases basal and IGF-1-stimulated myotube growth, respectively. PHGDH was of interest to us because β2-agonist-mediated muscle hypertrophy increases the mRNA and protein levels of PHGDH in pigs [33], and *Phgdh* expression almost doubles when muscle hypertrophy is stimulated through synergist ablation in mice (reanalysis of data from Ref. [9]). Our data indicate that PHGDH not only limits cellular proliferation [29] but also the size of post-mitotic muscle cells. This might seem surprising, as PHGDH catalyses the de novo synthesis of a non-essential amino acid; thus, one might assume that the loss of PHGDH would have little impact so long as dietary serine intake is sufficient. However, a complete loss of *Phgdh* is embryonal lethal in mice [56]. PHGDH mutations in humans also cause severe inborn diseases, such as Neu-Laxova syndrome [57], which is associated with atrophic or underdeveloped skeletal muscles [58]. The importance of PHGDH for normal development and muscle size regulation could be explained through serine's role as a key metabolite for one-carbon metabolism, which is linked to nucleotide and amino acid synthesis, epigenetics, and redox defence [27,28]. A metabolomics analysis showed that PHGDH is required to maintain nucleotide synthesis [28] and, hence, might affect RNA and ribosome biogenesis in muscle cells. Another mechanism through which PHGDH possibly regulates muscle size in vivo is via alpha-ketoglutarate (AKG). This metabolite is generated downstream of PHGDH and is diminished ≈50 % upon PHGDH knockdown [29]. Muscle concentrations of AKG are elevated after resistance exercise and AKG supplementation increases lean body mass in mice [59]. Future studies should seek to identify the mechanisms by which PHGDH contributes to post-mitotic muscle homeostasis and growth.

The fifth finding of this study is that AKT regulates PHGDH expression in C2C12 myotubes (Fig. 6). Further investigation is needed to assess whether PHGDH also increases in mice where overexpression of AKT causes muscle hypertrophy [45], and whether the reduction of PHGDH in these models or in other models of PHDGH activity/expression-associated hypertrophy [9] attenuates muscle size.

Several additional questions remain unanswered. First, our study only reports in vitro data obtained by studying C2C12 and primary mouse myotubes. Whilst both C2C12 myotubes [25,35,60] and mouse muscles respond to IGF-1 with hypertrophy [61], it is unclear whether in vivo hypertrophy involves the same metabolic reprogramming that we report here. Second, whilst mRNA markers of myogenesis [62] and myonuclear fusion [63] of C2C12 cells peak at day 3 of differentiation, we cannot exclude the possibility that myotubes were still undergoing differentiation-related myofibrillar growth at the time of gain/loss-of-function and compound experiments. Thus, some reported effects may represent an interaction between myotube differentiation and treatment. Third, although ^{14}C is incorporated into protein (Fig. 1d and e), future studies should use de-glycosylation treatments to delineate the extent to which this is because glucose is used as a substrate for amino acids-to-protein synthesis versus post-translational modification (i.e. glycosylation) of proteins [64].

5. Conclusions

Here we provide evidence that glycolysis is important in growing C2C12 and primary mouse myotubes. Reminiscent of cancer-like

metabolic reprogramming, this glycolysis-for-anabolism metabolic shift critically determines typical myotube size and IGF-1-stimulated muscle growth, at least in part through PHGDH.

Funding

Brendan M. Gabriel was supported by fellowships from the Novo Nordisk Foundation (NNF19OC0055072) & the Wenner-Gren Foundation, an Albert Renold Travel Fellowship from the European Foundation for the Study of Diabetes, and an Eric Reid Fund for Methodology from the Biochemical Society. **Abdalla D. Mohamed** was funded initially by Sarcoma UK (grant number SUK09.2015), then supported by funding from Postdoctoral Fellowship Program (Helmholtz Zentrum München, Germany), and currently by Cancer Research UK.

Institutional review board statement

The experiments on primary cells were conducted with post-mortem material from surplus mice (C57BL/6 J) originating from breeding excess that had to be terminated in the animal facility, and therefore, these animals do not fall under the Netherlands Law on Animal Research in agreement with the Directive 2010/63/EU.

Availability of data and material

The data that support the findings of this study are openly available in figshare at https://doi.org/10.6084/m9.figshare.20182214.

CRediT authorship contribution statement

Lian E.M. Stadhouders: Writing – review & editing, Writing – original draft, Visualization, Methodology, Investigation, Formal analysis, Data curation, Conceptualization. **Jonathon A.B. Smith:** Writing – review & editing, Visualization, Methodology, Investigation, Formal analysis. **Brendan M. Gabriel:** Writing – review & editing, Methodology, Investigation, Funding acquisition, Formal analysis. **Sander A.J. Verbrugge:** Writing – review & editing, Writing – original draft, Visualization, Formal analysis, Data curation. **Tim D. Hammersen:** Visualization, Methodology, Investigation, Formal analysis. **Detmar Kolijn:** Visualization, Methodology, Investigation, Formal analysis. **Ilse S.P. Vogel:** Writing – review & editing, Methodology, Investigation, Formal analysis. **Abdalla D. Mohamed:** Writing – review & editing, Resources, Funding acquisition. **Gerard M.J. de Wit:** Methodology, Investigation, Formal analysis. **Carla Offringa:** Methodology, Investigation, Formal analysis. **Willem M.H. Hoogaars:** Writing – review & editing, Resources, Methodology. **Sebastian Gehlert:** Writing – review & editing, Supervision, Resources, Project administration, Funding acquisition, Conceptualization. **Henning Wackerhage:** Writing – review & editing, Writing – original draft, Visualization, Supervision, Resources, Project administration, Funding acquisition, Conceptualization. **Richard T. Jaspers:** Writing – review & editing, Writing – original draft, Visualization, Supervision, Resources, Project administration, Funding acquisition, Conceptualization.

Declaration of competing interest

The authors declare that they have no known competing financial interests or personal relationships that could have influenced the work reported in this paper.

Data availability

The data that support the findings of this study are openly available in figshare at DOI: 10.6084/m9.figshare.20182214

References

[1] B.M. Gabriel, J.R. Zierath, The limits of exercise Physiology: from performance to health, Cell Metabol. 25 (5) (2017) 1000–1011.
[2] R.R. Wolfe, The underappreciated role of muscle in health and disease, Am. J. Clin. Nutr. 84 (3) (2006) 475–482.
[3] N.K. Arden, T.D. Spector, Genetic influences on muscle strength, lean body mass, and bone mineral density: a twin study, J. Bone Miner. Res. 12 (12) (1997) 2076–2081.
[4] S.A.J. Verbrugge, M. Schonfelder, L. Becker, F. Yaghoob Nezhad, M. Hrabe de Angelis, H. Wackerhage, Genes whose gain or loss-of-function increases skeletal muscle mass in mice: a systematic literature review, Front. Physiol. 9 (2018) 553.
[5] J.P. Ahtiainen, S. Walker, H. Peltonen, J. Holviala, E. Sillanpaa, L. Karavirta, et al., Heterogeneity in resistance training-induced muscle strength and mass responses in men and women of different ages, Age (Dordr) 38 (1) (2016) 10.
[6] C. McGlory, M.C. Devries, S.M. Phillips, Skeletal muscle and resistance exercise training; the role of protein synthesis in recovery and remodeling, J. Appl. Physiol. 122 (3) (1985) 541–548, 2017.
[7] B.F. Miller, J.L. Olesen, M. Hansen, S. Dossing, R.M. Crameri, R.J. Welling, et al., Coordinated collagen and muscle protein synthesis in human patella tendon and quadriceps muscle after exercise, J. Physiol. 567 (Pt 3) (2005) 1021–1033.
[8] C.A. Goodman, Role of mTORC1 in mechanically induced increases in translation and skeletal muscle mass, J. Appl. Physiol. 127 (2) (1985) 581–590, 2019.
[9] T. Chaillou, J.D. Lee, J.H. England, K.A. Esser, J.J. McCarthy, Time course of gene expression during mouse skeletal muscle hypertrophy, J. Appl. Physiol. 115 (7) (1985) 1065–1074, 2013.
[10] N.J. Pillon, B.M. Gabriel, L. Dollet, J.A.B. Smith, L. Sardon Puig, J. Botella, et al., Transcriptomic profiling of skeletal muscle adaptations to exercise and inactivity, Nat. Commun. 11 (1) (2020) 470.
[11] K. Vissing, P. Schjerling, Simplified data access on human skeletal muscle transcriptome responses to differentiated exercise, Sci. Data 1 (2014), 140041.
[12] M.S. Lawrence, P. Stojanov, P. Polak, G.V. Kryukov, K. Cibulskis, A. Sivachenko, et al., Mutational heterogeneity in cancer and the search for new cancer-associated genes, Nature 499 (7457) (2013) 214–218.
[13] R.J. DeBerardinis, N.S. Chandel, Fundamentals of cancer metabolism, Sci. Adv. 2 (5) (2016), e1600200.
[14] O. Warburg, F. Wind, E. Negelein, The metabolism of tumors in the body, J. Gen. Physiol. 8 (6) (1927) 519–530.
[15] E. Racker, Bioenergetics and the problem of tumor growth, Am. Sci. 60 (1) (1972) 56–63.
[16] E. Gaude, C. Frezza, Tissue-specific and convergent metabolic transformation of cancer correlates with metastatic potential and patient survival, Nat. Commun. 7 (1) (2016), 13041.
[17] H. Wackerhage, I.J. Vechetti, P. Baumert, S. Gehlert, L. Becker, R.T. Jaspers, et al., Does a hypertrophying muscle fibre reprogramme its metabolism similar to a cancer cell? Sports Med. 52 (11) (2022) 2569–2578.
[18] F. Fathinul, W. Lau, Avid F-FDG uptake of pectoralis major muscle: an equivocal sequela of strenuous physical exercise, Biomed. Imaging Interv. J. 5 (2) (2009) e7.
[19] R.L. Marcus, O. Addison, P.C. LaStayo, R. Hungerford, A.R. Wende, J.M. Hoffman, et al., Regional muscle glucose uptake remains elevated one week after cessation of resistance training independent of altered insulin sensitivity response in older adults with type 2 diabetes, J. Endocrinol. Invest. 36 (2) (2013) 111–117.
[20] C. Semsarian, P. Sutrave, D.R. Richmond, R.M. Graham, Insulin-like growth factor (IGF-I) induces myotube hypertrophy associated with an increase in anaerobic glycolysis in a clonal skeletal-muscle cell model, Biochem. J. 339 (Pt 2) (1999) 443–451. Pt 2.
[21] R.L. Elstrom, D.E. Bauer, M. Buzzai, R. Karnauskas, M.H. Harris, D.R. Plas, et al., Akt stimulates aerobic glycolysis in cancer cells, Cancer Res. 64 (11) (2004) 3892–3899.
[22] Y. Izumiya, T. Hopkins, C. Morris, K. Sato, L. Zeng, J. Viereck, et al., Fast/Glycolytic muscle fiber growth reduces fat mass and improves metabolic parameters in obese mice, Cell Metabol. 7 (2) (2008) 159–172.
[23] P.A. Dutchak, S.J. Estill-Terpack, A.A. Plec, X. Zhao, C. Yang, J. Chen, et al., Loss of a negative regulator of mTORC1 induces aerobic glycolysis and altered fiber composition in skeletal muscle, Cell Rep. 23 (7) (2018) 1907–1914.
[24] E. Mouisel, K. Relizani, L. Mille-Hamard, R. Denis, C. Hourde, O. Agbulut, et al., Myostatin is a key mediator between energy metabolism and endurance capacity of skeletal muscle, Am. J. Physiol. Regul. Integr. Comp. Physiol. 307 (4) (2014) R444–R454.
[25] S.A.J. Verbrugge, S. Gehlert, L.E.M. Stadhouders, D. Jacko, T. Aussieker, MJdW. G, et al., PKM2 determines myofiber hypertrophy in vitro and increases in response to resistance exercise in human skeletal muscle, Int. J. Mol. Sci. 21 (19) (2020).
[26] P. Baumert, S. Mäntyselkä, M. Schönfelder, M. Heiber, A. Swaminathan, P. Minderis, et al., Skeletal muscle hypertrophy rewires glucose metabolism in mice: an experimental investigation and systematic review, bioRxiv (2022), https://doi.org/10.1101/2022.12.08.519580.
[27] G.S. Ducker, J.D. Rabinowitz, One-carbon metabolism in health and disease, Cell Metabol. 25 (1) (2017) 27–42.
[28] M.A. Reid, A.E. Allen, S. Liu, M.V. Liberti, P. Liu, X. Liu, et al., Serine synthesis through PHGDH coordinates nucleotide levels by maintaining central carbon metabolism, Nat. Commun. 9 (1) (2018) 5442.
[29] R. Possemato, K.M. Marks, Y.D. Shaul, M.E. Pacold, D. Kim, K. Birsoy, et al., Functional genomics reveal that the serine synthesis pathway is essential in breast cancer, Nature 476 (7360) (2011) 346–350.

[30] S. Vandekeere, C. Dubois, J. Kalucka, M.R. Sullivan, M. Garcia-Caballero, J. Goveia, et al., Serine synthesis via PHGDH is essential for heme production in endothelial cells, Cell Metabol. 28 (4) (2018) 573–587 e13.
[31] M. Hamano, T. Sayano, W. Kusada, H. Kato, S. Furuya, Microarray data on altered transcriptional program of Phgdh-deficient mouse embryonic fibroblasts caused by L-serine depletion, Data Brief 7 (2016) 1598–1601.
[32] J.G. Ryall, S. Dell'Orso, A. Derfoul, A. Juan, H. Zare, X. Feng, et al., The NAD(+)-dependent SIRT1 deacetylase translates a metabolic switch into regulatory epigenetics in skeletal muscle stem cells, Cell Stem Cell 16 (2) (2015) 171–183.
[33] D.M. Brown, H. Williams, K.J. Ryan, T.L. Wilson, Z.C. Daniel, M.H. Mareko, et al., Mitochondrial phosphoenolpyruvate carboxykinase (PEPCK-M) and serine biosynthetic pathway genes are co-ordinately increased during anabolic agent-induced skeletal muscle growth, Sci. Rep. 6 (1) (2016), 28693.
[34] A.U. Trendelenburg, A. Meyer, D. Rohner, J. Boyle, S. Hatakeyama, D.J. Glass, Myostatin reduces Akt/TORC1/p70S6K signaling, inhibiting myoblast differentiation and myotube size, Am. J. Physiol. Cell Physiol. 296 (6) (2009) C1258–C1270.
[35] C. Rommel, S.C. Bodine, B.A. Clarke, R. Rossman, L. Nunez, T.N. Stitt, et al., Mediation of IGF-1-induced skeletal myotube hypertrophy by PI(3)K/Akt/mTOR and PI(3)K/Akt/GSK3 pathways, Nat. Cell Biol. 3 (11) (2001) 1009–1013.
[36] J.S. You, R.M. McNally, B.L. Jacobs, R.E. Privett, D.M. Gundermann, K.H. Lin, et al., The role of raptor in the mechanical load-induced regulation of mTOR signaling, protein synthesis, and skeletal muscle hypertrophy, Faseb. J. 33 (3) (2019) 4021–4034.
[37] N.D. Steinert, G.K. Potts, G.M. Wilson, A.M. Klamen, K.H. Lin, J.B. Hermanson, et al., Mapping of the contraction-induced phosphoproteome identifies TRIM28 as a significant regulator of skeletal muscle size and function, Cell Rep. 34 (9) (2021), 108796.
[38] H. Xi, M. Kurtoglu, T.J. Lampidis, The wonders of 2-deoxy-D-glucose, IUBMB Life 66 (2) (2014) 110–121.
[39] G.R. Steinberg, D.G. Hardie, New insights into activation and function of the AMPK, Nat. Rev. Mol. Cell Biol. 24 (4) (2023) 255–272.
[40] P.J. Atherton, J. Babraj, K. Smith, J. Singh, M.J. Rennie, H. Wackerhage, Selective activation of AMPK-PGC-1 alpha or PKB-TSC2-mTOR signaling can explain specific adaptive responses to endurance or resistance training-like electrical muscle stimulation, Faseb. J. 19 (7) (2005) 786–788.
[41] R. Sartori, V. Romanello, M. Sandri, Mechanisms of muscle atrophy and hypertrophy: implications in health and disease, Nat. Commun. 12 (1) (2021) 330.
[42] G. Leprivier, B. Rotblat, How does mTOR sense glucose starvation? AMPK is the usual suspect, Cell Death Dis. 6 (1) (2020) 27.
[43] B.T. O'Neill, K.Y. Lee, K. Klaus, S. Softic, M.T. Krumpoch, J. Fentz, et al., Insulin and IGF-1 receptors regulate FoxO-mediated signaling in muscle proteostasis, J. Clin. Invest. 126 (9) (2016) 3433–3446.
[44] L. Jacobsen, S. Calvin, E. Lobenhofer, Transcriptional effects of transfection: the potential for misinterpretation of gene expression data generated from transiently transfected cells, Biotechniques 47 (1) (2009) 617–624.
[45] K.M. Lai, M. Gonzalez, W.T. Poueymirou, W.O. Kline, E. Na, E. Zlotchenko, et al., Conditional activation of akt in adult skeletal muscle induces rapid hypertrophy, Mol. Cell Biol. 24 (21) (2004) 9295–9304.
[46] A.M. Hosios, V.C. Hecht, L.V. Danai, M.O. Johnson, J.C. Rathmell, M. L. Steinhauser, et al., Amino acids rather than glucose account for the majority of cell mass in proliferating mammalian cells, Dev. Cell 36 (5) (2016) 540–549.
[47] A.J. Garber, I.E. Karl, D.M. Kipnis, Alanine and glutamine synthesis and release from skeletal muscle. II. The precursor role of amino acids in alanine and glutamine synthesis, J. Biol. Chem. 251 (3) (1976) 836–843.
[48] T.A. Churchward-Venne, N.A. Burd, C.J. Mitchell, D.W. West, A. Philp, G. R. Marcotte, et al., Supplementation of a suboptimal protein dose with leucine or essential amino acids: effects on myofibrillar protein synthesis at rest and following resistance exercise in men, J. Physiol. 590 (11) (2012) 2751–2765.
[49] J. Lee, D. Kim, C. Kim, Resistance training for glycemic control, muscular strength, and lean body mass in old type 2 diabetic patients: a meta-analysis, Diabetes Ther 8 (3) (2017) 459–473.
[50] V. Tixier, L. Bataille, C. Etard, T. Jagla, M. Weger, J.P. Daponte, et al., Glycolysis supports embryonic muscle growth by promoting myoblast fusion, Proc. Natl. Acad. Sci. U. S. A. 110 (47) (2013) 18982–18987.
[51] J.F. Tong, X. Yan, M.J. Zhu, M. Du, AMP-activated protein kinase enhances the expression of muscle-specific ubiquitin ligases despite its activation of IGF-1/Akt signaling in C2C12 myotubes, J. Cell. Biochem. 108 (2) (2009) 458–468.
[52] M.N. Lee, S.H. Ha, J. Kim, A. Koh, C.S. Lee, J.H. Kim, et al., Glycolytic flux signals to mTOR through glyceraldehyde-3-phosphate dehydrogenase-mediated regulation of Rheb, Mol. Cell Biol. 29 (14) (2009) 3991–4001.
[53] J.L. Andersen, P. Aagaard, Myosin heavy chain IIX overshoot in human skeletal muscle, Muscle Nerve 23 (7) (2000) 1095–1104.
[54] P.L. Kim, R.S. Staron, S.M. Phillips, Fasted-state skeletal muscle protein synthesis after resistance exercise is altered with training, J. Physiol. 568 (Pt 1) (2005) 283–290.
[55] T. van Wessel, A. de Haan, W.J. van der Laarse, R.T. Jaspers, The muscle fiber type-fiber size paradox: hypertrophy or oxidative metabolism? Eur. J. Appl. Physiol. 110 (4) (2010) 665–694.
[56] K. Yoshida, S. Furuya, S. Osuka, J. Mitoma, Y. Shinoda, M. Watanabe, et al., Targeted disruption of the mouse 3-phosphoglycerate dehydrogenase gene causes severe neurodevelopmental defects and results in embryonic lethality, J. Biol. Chem. 279 (5) (2004) 3573–3577.
[57] R. Shaheen, Z. Rahbeeni, A. Alhashem, E. Faqeih, Q. Zhao, Y. Xiong, et al., Neu-Laxova syndrome, an inborn error of serine metabolism, is caused by mutations in PHGDH, Am. J. Hum. Genet. 94 (6) (2014) 898–904.
[58] I.A. Shved, G.I. Lazjuk, E.D. Cherstvoy, Elaboration of the phenotypic changes of the upper limbs in the Neu-Laxova syndrome, Am. J. Med. Genet. 20 (1) (1985) 1–11.
[59] Y. Yuan, P. Xu, Q. Jiang, X. Cai, T. Wang, W. Peng, et al., Exercise-induced alpha-ketoglutaric acid stimulates muscle hypertrophy and fat loss through OXGR1-dependent adrenal activation, EMBO J. 39 (7) (2020), e103304.
[60] E.L. Peters, S.M. van der Linde, I.S.P. Vogel, M. Haroon, C. Offringa, G.M.J. de Wit, et al., IGF-1 attenuates hypoxia-induced atrophy but inhibits myoglobin expression in C2C12 skeletal muscle myotubes, Int. J. Mol. Sci. 18 (9) (2017).
[61] A. Musaro, K. McCullagh, A. Paul, L. Houghton, G. Dobrowolny, M. Molinaro, et al., Localized Igf-1 transgene expression sustains hypertrophy and regeneration in senescent skeletal muscle, Nat. Genet. 27 (2) (2001) 195–200.
[62] A.M. Abdelmoez, L. Sardon Puig, J.A.B. Smith, B.M. Gabriel, M. Savikj, L. Dollet, et al., Comparative profiling of skeletal muscle models reveals heterogeneity of transcriptome and metabolism, Am. J. Physiol. Cell Physiol. 318 (3) (2020) C615–C626.
[63] N. Yoshida, S. Yoshida, K. Koishi, K. Masuda, Y. Nabeshima, Cell heterogeneity upon myogenic differentiation: down-regulation of MyoD and Myf-5 generates 'reserve cells', J. Cell Sci. 111 (Pt 6) (1998) 769–779.
[64] K. Marino, J. Bones, J.J. Kattla, P.M. Rudd, A systematic approach to protein glycosylation analysis: a path through the maze, Nat. Chem. Biol. 6 (10) (2010) 713–723.